† Electronic supplementary information (ESI)

Livestock manure improved antibiotic resistance gene removal during co-treatment of domestic wastewater in an anaerobic membrane bioreactor

Esther Lou[a], Moustapha Harb[b], Adam L. Smith[c], and Lauren B. Stadler[a,*]

[a] Department of Civil and Environmental Engineering, Rice University, 6100 Main Street, MS 519, Houston, TX 77005
[b] Department of Civil and Environmental Engineering, Lebanese American University, 309 Bassil Building, Byblos, Lebanon 2038-1401
[c] Astani Department of Civil and Environmental Engineering, University of Southern California, 3620 South Vermont Avenue, Los Angeles, CA 90089, USA
*Corresponding author: Lauren B. Stadler, Department of Civil and Environmental Engineering, Rice University, 6100 Main Street, MS 519, Houston, TX 77005
E-mail address: Esther Lou (esther.lou@rice.edu), Lauren B. Stadler (lauren.stadler@rice.edu)

1. Methods

1.1 AnMBR set-up and monitoring

1.1.1 AnMBR configuration and operational parameters

The AnMBR with a liquid volume of 4.5 L (Chemglass Life Science, Vineland, NJ) was operated continuously. The hydraulic retention time (HRT) of the AnMBR was maintained at 19 h by controlling the membrane permeate flux. Biomass was only removed from the AnMBR for sampling purposes, resulting in a solids retention time (SRT) of >300 days. Headspace gas was recirculated using a diaphragm pump (KNF Neuberger, Trenton, NJ), and then distributed below each membrane through a horizontally placed sparging tube designed for fouling control. The gas flow rate passing through each sparging tube was controlled via a gas flow meter to maintain the TMPs of all three membranes similar to one another and below 5.5 kPa. The TMP across each membrane was measured using a pressure transducer (Omega Engineering, Stamford, CT). The headspace pressure was monitored using another pressure transducer and the biogas was collected using a Tedlar sampling bag attached to the head plate (Restek, Bellefonte, PA) after a check valve. The influent was stored in a 4 °C refrigerator and pumped into the reactor through a peristaltic pump (Cole-Parmer, Vernon Hills, IL). The effluent was continuously withdrawn with another peristaltic pump with a backwash ratio of 10%. The liquid level was monitored by a sensor switch. The AnMBR was connected to a computer, which operated a control program and LabVIEW (National Instruments, Austin, TX) data acquisition software. The control program was responsible for operation of all pumps, biogas recirculation, and mixing. The LabVIEW 2017 software (Student Edition)

23 continuously monitored and recorded temperature, TMPs, feed flow rate, and head space
24 pressure.

25 **1.1.2 Operation stages and feeding preparation**

26 After inoculation, the AnMBR fed treating domestic wastewater for 3 weeks until it
27 reached steady-state operation (defined as headspace biogas methane content > 60% and
28 effluent COD < 50 mg/L treating domestic wastewater). Baseline stage commenced 121
29 days after the AnMBR was started up. The duration of each operational stage was: 16 days
30 (Baseline), 20 days (Stage 1), 15 days (Stage 2), 17 days (Stage 3), and 18 days (Stage 4).
31 In each operational stage, samples were collected approximately every 2 HRTs. The
32 influent for Stages 1 - 4 was prepared by defrosting frozen manure slurry in the fridge,
33 homogenizing the manure slurry with a Waring Blender, weighing the slurry, and mixing it
34 with freshly collected domestic wastewater. After adding the manure to the wastewater, the
35 influent was then passed through a 1 mm sieve to remove large solids and prevent influent
36 channel clogging.

37 Biogas was collected in Tedlar sampling bags with valve and septum fittings
38 (Restek, PA) through a built-in port to the reactor headspace. The volume of biogas
39 produced was measured using a 100 mL BD Slip Tip syringe connected to the gas bag
40 valve after the gas bag had been inflated for approximately a day. A one-way check valve
41 was place between the headspace and the sampling bag to prevent leaking during sampling.
42 For quantitative analysis of the biogas composition, biogas was sampled using a gas-tight
43 glass syringe with lock (Hamilton) and assessed by TRACE™ 1300 Gas Chromatograph
44 (ThermoFisher Scientific) with pulsed discharge detector (GC-PDD). The standard curve
45 for methane quantification was prepared using analytical grade methane (Airgas).

Chemical oxygen demand (COD) was measured in accordance with USEPA Method 410.4 using Genesys 10S UV-Vis Spectrophotometer (Thermo Scientific) and COD vial kits (CHEMetrics Inc.). Volatile fatty acids (acetate, propionate, formate and valerate), sulfate and nitrate were measured by ion chromatography on an ICS 2100 (Thermo Fisher Scientific, Waltham, MA) using methods described previously.[1]

1.2 DNA extraction with internal standards

Internal standards of cell-associated DNA (caDNA) and cell-free DNA (cfDNA) were spiked into samples prior to filtration and DNA extraction to correct for losses during sample processing and DNA extraction. For the caDNA internal standard, we spiked in *Escherichia. coli* DH10β containing an engineered plasmid. The plasmid, *pReporter_8* (RRID: Addgene_60568), is a low-copy plasmid that was previously modified by knocking out the gene encoding green fluorescence reporter (GFP) and replacing it with the methyl-halide transferase (MHT) gene found in *Batis Maritima.*[2] Prior to spiking the samples with the caDNA internal standard, *E. coli* DH10β was grown up on a Luria broth plate containing 34 μg/mL chloramphenicol at 37 °C overnight. A single colony was transferred to a tube containing 2 mL Luria broth with 34 μg/mL chloramphenicol followed by incubation at 200 rpm under 37 °C. After 12 h of incubation, 500 μL liquid culture was added to influent and effluent samples, respectively, right before sample filtration. qPCR was performed on the samples spiked with internal standards to determine the copy number of the recovered caDNA internal standard in the final DNA extracts (C_i in equation 1) and the copy number of target genes in the final DNA extracts (C_s in equation 1). In addition, a 500 μL aliquot of liquid culture from the same culture tube of internal standard was used in

68 an independent DNA extraction to determine the copy number of caDNA internal standard
69 that was spiked into the sample (C_o in equation 1).
70 Before DNA extraction, membranes were cut to small pieces and transferred to
71 Lysing Matrix E tubes (MP Biomedicals). All Lysing Matrix E tubes (containing either
72 influent sample, effluent sample or the caDNA internal standards) underwent bead-beating
73 with the maximum intensity for 2 minutes (BioSpec Products, Mini-bead beater 24, 115 V).
74 After bead-beating, DNA extraction was performed using FastDNA SPIN Kit for Soil (MP
75 Biomedicals) and each sample was eluted to obtain a final volume of 100 μL of DNA
76 extract.
77 Plasmid pUC19 with an inserted sequence for qPCR was used as the internal
78 standard for cell-free ARG calibration. The insertion is a 183 bp fragment on *ARHGAP11B*
79 gene, a human-associated gene that is specific to the brain neocortex.[3] The DNA fragment
80 was synthesized (gBlocks, Integrated DNA technology Inc.) and cloned into pMini T2.0
81 vector and then transferred to NEB 10-β Competent *E. coli* using the PCR Cloning Kit
82 (New England BioLabs Inc., MA). Plasmids were extracted using ZR Plasmid Miniprep kit
83 (ZYMO Research, CA). Approximately 1×10^8 copies of synthesized pMini T2.0 plasmids
84 were added to each effluent sample prior to sample filtration and DNA extraction. The
85 quality of all DNA extracts was tested using 1000 UV-Vis Spectrophotometer
86 (ThermoFisher Scientific, MA). Qubit 3.0 fluorometer and Qubit dsDNA BR Assay Kit
87 (Invitrogen, CA) were applied for DNA quantification.
88 **1.3 Quantifications of target genes and internal standards in real time qPCR**
89 For all target genes (*sul*1, *sul*2, *tet*(W), *tet*(O), *ampC*, *ermB*, *ermF*, *blaOXA-1*, *blaNDM1*,
90 *tp614*, *intI1*) as well as caARG and cfARG internal standards, 10.5 uL qPCR reactions

were performed on MicroAmp Fast Optical 96-Well Reaction Plate (0.1 mL, Applied Biosystems) using the QuantStudio 3.0 Real-Time PCR Systems (Applied Biosystems, CA). The standard amplification protocol consisted of an initial denaturation step at 95 °C for 2 min, followed by 40 amplification cycles at 95 °C for 5 s, annealing temperature for 12 s, and 72 °C for 16 s and the melting steps (at 95 °C for 15 s, 60 °C for 1 min, at 95 °C for 15 s). qPCR standards were prepared by inserting the target genes into pMiniT 2.0 vector and transformed to NEB 10-β Competent E. coli using the NEB PCR Cloning Kit (New England Biolabs, MA). The inserted target genes, before cloning and transformation, were purified and sequenced PCR products of the AnMBR sludge. The PCR assays were conducted using the exact same primers and conditions as the qPCR assays in this study. In addition, PCR products were analyzed on 1% agarose gel electrophoresis to verify the correct amplicon size and the negative presence of non-specific products. The expected PCR products were then cut off from the gel, purified by a Qiagen QIAquick Gel Extraction kit, and sequenced by Sanger method (Genewiz, Inc., TX) to confirm the sequences. After cloning and transformation, transformed *E. coli* were selected for on AMP selection plates. Grown single colony was picked and cultured overnight again in AMP selection LB overnight. Plasmid extraction was then conducted to acquire plasmids from the cell culture using a ZR Plasmid Miniprep kit (ZYMO Research, CA). Extracted plasmids were then diluted ten-fold to generate standard curve for each qPCR assay. For all qPCR assays performed in this study, three technical replicates were conducted for each biological replicate, melt curves were checked for all reactions, and 3 NTCs were included on each plate. qPCR reaction efficiencies and limits of quantification (lowest standard concentration; LOQ) for each assay are reported in ESI Table S5.

2. Results

2.1 Performance

The performance of the AnMBR across all operational stages is shown in Figure A2. In addition, ion-chromatography results showed trace concentration of formic acid (2.21 ± 0.18 mg/L) and acetic acid (2.72 ± 0.16 mg/L) in the effluent during Baseline operation. With the addition of manure starting from Stage 1, effluent COD gradually increased (Fig. S1). Interestingly, in the effluent of Baseline operation, propionate was not detected; however, from Stage 1 through 4, propionate started to accumulate in the effluent significantly due to the addition of manure ($p<0.01$). Previous studies have shown propionate is a key indicator denoting process imbalances in anaerobic digesters treating complex organic waste,[4,5] which is consistent with the input of manure starting from Stage 1. VFA concentrations are listed in ESI† Table S2. Solids concentrations are listed in ESI† Table S1.

2.2 The absolute and relative concentrations of target genes in influent and effluent across stages

The DNA recoveries are shown in Table S6. cfDNA recovery efficiencies for all stages averaged approximately 30% and were consistent across stages. While the average recovery efficiency was lower than the >90% recovery reported by the group that developed the method,[6] the discrepancy is likely due to differences in experimental steps used during cfDNA extraction. Specifically, Wang et al. only attempted to recover cfDNA without also recovering caDNA. In contrast, we first processed the samples to collect caDNA using filtration, and then used the filtrate to capture the cfDNA using absorption-elution. As a result, a fraction of cfDNA may have been lost during filtration. Our reported

recoveries were nevertheless higher than other widely-applied methods for cfDNA such as alcohol precipitation and CTAB-based extraction and commercial kits (recovery efficiencies typically <10%).[7–9] In addition, the recoveries in this study were consistent across all stages (Table. S6), reflecting the reproducibility of the applied cfDNA extraction protocol. As the goal of using internal standards for tracking recoveries is to calibrate target gene abundance data, the reproducibility of DNA recovery is as important, if not more so, than a high recovery value.

2.3 Correlation analysis of effluent cell-associated and cell-free ARGs

Correlation analysis of effluent caARGs revealed significant associations between different gene types. Effluent cell-associated *intI1* concentrations were significantly positively correlated with *sul1* concentrations across all stages of treatment (Pearsons, $r = 0.97$, $p < 0.01$). This suggests *sul1* may be associated with a Class I integron cassette and co-located on the same plasmids, which was consistent with previous studies on ARG fate in different environments.[10–12] The correlation between *intI1* and *sul1* is not surprising because they are both associated with Class I integrons.[13,14] We also observed that the cell-associated concentrations of *ampC* were positively correlated with *rpoB* concentrations (Pearsons $r = 0.91$, $p < 0.01$) indicating *ampC* genes are likely cell-associated, which is consistent with the fact that *ampC* genes are frequently detected on chromosomes.[15,16]

We observed that *intI1* only correlated with one other ARG (*sul1*) in the cell-associated DNA fraction, but strongly positively correlated with multiple ARGs in the cell-free fraction: *sul2* (Pearons, $r = 0.58$, $p < 0.01$), *ampC* (Pearsons, $r = 0.63$, $p < 0.01$) and *ermB* (Pearsons, $r = 0.89$, $p < 0.01$). These results are in contrast to some previous studies on fate of ARGs in wastewater environments that reported insignificant associations

between *intI1* and *sul2*, whereas they observed significant positive associations between *intI1* and *sul1*.[17–20] However, in soil and manure environments, significant positive associations between *intI1* and *sul2* have been frequently observed.[11,21–26] *IntI1* has drawn attention in many research studies because it is a proxy for anthropogenic pollution including antibiotic resistance dissemination.[27] However, it is challenging to compare our data to these previous studies directly because neither did they explicitly distinguish the cfARGs from caARGs, nor even capture the cfARG fraction due to the methods they used.[28–31]

The concentrations of cell-free *blaOXA-1*, *tp614* and *blaNDM1* in the effluent increased consistently across all stages (t-test, $p < 0.05$; Fig. 4B). The enrichment of *tp614* has also been reported in several wastewater treatment processes,[32] which underscores the challenge of removing it. The difficulty in removing *tp614* is noteworthy because its concentration has been found to positively correlate with persistent ARGs, particularly tetracycline and extended spectrum beta-lactamase (ESBL) ARGs.[33] We also observed a significant and positive correlation between *tp614* and *blaOXA-1* (Pearsons, $r = 0.98$, $p < 0.01$), and *tp614* and *ermF* (Pearsons, $r = 0.97$, $p < 0.01$). The detailed correlation analysis data using Pearson's correlation analysis can be found in Tables S11 and S12.

References

1. Chen S, Smith AL. Methane-driven microbial fuel cells recover energy and mitigate dissolved methane emissions from anaerobic effluents. Environ Sci Water Res Technol. 2018,**4**,67–79.
2. Cheng HY, Masiello CA, Bennett GN, Silberg JJ. Volatile Gas Production by Methyl Halide Transferase: An in Situ Reporter of Microbial Gene Expression in Soil. Environ Sci Technol. 2016,**50**,8750–9.
3. Florio M, Albert M, Taverna E, Namba T, Brandl H, Lewitus E, et al. Human-specific gene ARHGAP11B promotes basal progenitor amplification and neocortex expansion. Science (80-). 2015,.
4. Zitomer D, Maki J, Venkiteshwaran K, Bocher B. Relating Anaerobic Digestion Microbial Community and Process Function. Microbiol Insights. 2016,**8s2**,37.
5. Demirel B, Yenigün O. The effects of change in volatile fatty acid (vfa) composition on methanogenic upflow filter reactor (ufaf) performance. Environ Technol (United Kingdom). 2002,**23**,1179–87.
6. Wang DN, Liu L, Qiu ZG, Shen ZQ, Guo X, Yang D, et al. A new adsorption-elution technique for the concentration of aquatic extracellular antibiotic resistance genes from large volumes of water. Water Res. 2016,**92**,188–98.
7. Liang Z, Keeley A. Filtration recovery of extracellular DNA from environmental water samples. Environ Sci Technol. 2013,.
8. Eichmiller JJ, Miller LM, Sorensen PW. Optimizing techniques to capture and extract environmental DNA for detection and quantification of fish. Mol Ecol Resour. 2016,**16**,56–68.

9. Li F, Peng Y, Fang W, Altermatt F, Xie Y, Yang J, et al. Application of Environmental DNA Metabarcoding for Predicting Anthropogenic Pollution in Rivers. Environ Sci Technol. 2018,acs.est.8b03869.
10. Zarei-baygi A, Harb M, Wang P, Stadler LB, Smith AL. Evaluating Antibiotic Resistance Gene Correlations with Antibiotic Exposure Conditions in Anaerobic Membrane Bioreactors. Environ Sci Technol. 2019,**53**,3599–609.
11. Duan M, Gu J, Wang X, Li Y, Zhang S, Yin Y, et al. Effects of genetically modified cotton stalks on antibiotic resistance genes, intI1, and intI2 during pig manure composting. Ecotoxicol Environ Saf. 2018,**147**,637–42.
12. Xu Y, Guo C, Luo Y, Lv J, Zhang Y, Lin H, et al. Occurrence and distribution of antibiotics, antibiotic resistance genes in the urban rivers in Beijing, China. Environ Pollut. 2016,**213**,833–40.
13. Mazel D. Integrons: Agents of bacterial evolution. Nat Rev Microbiol. 2006,**4**,608–20.
14. Deng Y, Bao X, Ji L, Chen L, Liu J, Miao J, et al. Resistance integrons: class 1, 2 and 3 integrons. Ann Clin Microbiol Antimicrob. 2015,**14**,45.
15. Bergstrom S, Olsson O, Normark S. Common evolutionary origin of chromosomal beta-lactamase genes in enterobacteria. J Bacteriol. 1982,**150**,528–34.
16. Mata C, Miró E, Alvarado A, Garcillán-Barcia MP, Toleman M, Walsh TR, et al. Plasmid typing and genetic context of AmpC β-lactamases in enterobacteriaceae lacking inducible chromosomal ampC genes: Findings from a Spanish hospital 1999-2007. J Antimicrob Chemother. 2012,**67**,115–22.
17. Lu J, Zhang Y, Wu J, Wang J, Cai Y. Fate of antibiotic resistance genes in reclaimed

229 water reuse system with integrated membrane process. J Hazard Mater.
230 2020,**382**,121025.
231 18. Jang HM, Lee J, Choi S, Shin J, Kan E, Kim YM. Response of antibiotic and heavy
232 metal resistance genes to two different temperature sequences in anaerobic digestion
233 of waste activated sludge. Bioresour Technol. 2018,.
234 19. Ma L, Li AD, Yin X Le, Zhang T. The Prevalence of Integrons as the Carrier of
235 Antibiotic Resistance Genes in Natural and Man-Made Environments. Environ Sci
236 Technol. 2017,.
237 20. Li J, Cheng W, Xu L, Strong PJ, Chen H. Antibiotic-resistant genes and antibiotic-
238 resistant bacteria in the effluent of urban residential areas, hospitals, and a municipal
239 wastewater treatment plant system. Environ Sci Pollut Res. 2015,.
240 21. Sun W, Qian X, Gu J, Wang XJ, Duan ML. Mechanism and Effect of Temperature
241 on Variations in Antibiotic Resistance Genes during Anaerobic Digestion of Dairy
242 Manure. Sci Rep. 2016,**6**,1–9.
243 22. Liu P, Jia S, He X, Zhang X, Ye L. Different impacts of manure and chemical
244 fertilizers on bacterial community structure and antibiotic resistance genes in arable
245 soils. Chemosphere. 2017,**188**,455–64.
246 23. Guo X pan, Yang Y, Lu D pei, Niu Z shun, Feng J nan, Chen Y ru, et al. Biofilms as
247 a sink for antibiotic resistance genes (ARGs) in the Yangtze Estuary. Water Res.
248 2018,**129**,277–86.
249 24. Sun W, Gu J, Wang X, Qian X, Tuo X. Impacts of biochar on the environmental risk
250 of antibiotic resistance genes and mobile genetic elements during anaerobic digestion
251 of cattle farm wastewater. Bioresour Technol. 2018,**256**,342–9.

252 25. Zhao X, Wang J, Zhu L, Wang J. Field-based evidence for enrichment of antibiotic
253 resistance genes and mobile genetic elements in manure-amended vegetable soils.
254 Sci Total Environ. 2019,**654**,906–13.
255 26. Ma J, Gu J, Wang X, Peng H, Wang Q, Zhang R, et al. Effects of nano-zerovalent
256 iron on antibiotic resistance genes during the anaerobic digestion of cattle manure.
257 Bioresour Technol. 2019,**289**,121688.
258 27. Gillings MR, Gaze WH, Pruden A, Smalla K, Tiedje JM, Ku J. Using the class 1
259 integron-integrase gene as a proxy for anthropogenic pollution. ISME J.
260 2014,**9**,1269–79.
261 28. Zhang Y, Li H, Gu J, Qian X, Yin Y, Li Y, et al. Effects of adding different
262 surfactants on antibiotic resistance genes and intI1 during chicken manure
263 composting. Bioresour Technol. 2016,**219**,545–51.
264 29. Xu Y, Xu J, Mao D, Luo Y. Effect of the selective pressure of sub-lethal level of
265 heavy metals on the fate and distribution of ARGs in the catchment scale. Environ
266 Pollut. 2017,**220**,900–8.
267 30. Sun M, Ye M, Wu J, Feng Y, Wan J, Tian D, et al. Positive relationship detected
268 between soil bioaccessible organic pollutants and antibiotic resistance genes at dairy
269 farms in Nanjing, Eastern China. Environ Pollut. 2015,**206**,421–8.
270 31. Yuan Q Bin, Zhai YF, Mao BY, Hu N. Antibiotic resistance genes and intI1
271 prevalence in a swine wastewater treatment plant and correlation with metal
272 resistance, bacterial community and wastewater parameters. Ecotoxicol Environ Saf.
273 2018,**161**,251–9.
274 32. Yan W, Guo Y, Xiao Y, Wang S, Ding R, Jiang J, et al. The changes of bacterial

communities and antibiotic resistance genes in microbial fuel cells during long-term oxytetracycline processing. Water Res. 2018,**142**,105–14.

33. Jong MC, Su JQ, Bunce JT, Harwood CR, Snape JR, Zhu YG, et al. Co-optimization of sponge-core bioreactors for removing total nitrogen and antibiotic resistance genes from domestic wastewater. Sci Total Environ. 2018,**634**,1417–23.

Table S1 Solids contents in the influent, effluent and the mixed liquor.

Table S2 Volatile fatty acids (VFAs) concentrations in effluent across all operational stages.

Table S3 Internal standards for caARG and cfARG.

Table S4 Primer sequences and qPCR conditions for all target genes.

Table S5 qPCR reaction efficiencies and LOQs for each assay.

Table S6 caDNA and cfDNA recoveries of all stages.

Table S7 LRVs of genes across all stages.

Table S8 Concentrations of target genes in the influent across all stages (copies/mL of influent).

Table S9 Concentrations of targeted genes in the effluent across all stages (copies/mL of effluent) in the (a) Cell-associated fraction and (b) cell-free fraction.

Table S10 Relative abundance of ARGs and MGEs normalized by copies of *rpo*B in the influent and the effluent samples across all stages (copies/ copies of *rpo*B): a. influent; b. effluent.

Table S11 Correlation coefficients for target genes in the effluent cell-associated fraction across all stages, a. r values; b. corresponding p values.

Table S12 Correlation coefficients for target genes in the effluent cell-free fraction across all stages, a. r values; b. corresponding p-values.

Table S1 Solids contents in the influent, effluent and the mixed liquor (n=7).

	Baseline	Stage1	Stage2	Stage3	Stage4
Influent TSS (mg/L)	138.0 ± 2.40	5490 ± 104	8350 ± 164	13100 ± 262	20500 ± 405
Influent VSS (mg/L)	116.0 ± 2.33	4360 ± 85.1	6620 ± 134	10400 ± 208	16200 ± 322
Mixed liquor TSS (mg/L)	7550 ± 139	8240 ± 164	8690 ± 174	10600 ± 2110	12800 ± 256
Mixed liquor VSS (mg/L)	5510 ± 107	5930 ± 116	6430 ± 128	8150 ± 162	9720 ± 193

Table S2 Volatile fatty acids (VFAs) concentrations in effluent across all operational stages (n=4). The fraction of VFAs in effluent COD is calculated from the theoretical COD of VFAs normalized by the total effluent COD.

Operational Stage	Concentration of VFAs (mg/L)					The fraction of VFAs in effluent COD (%)
	Formate	Acetate	Propionate	Butyrate	Valerate	
Baseline	2.21 ± 0.18	2.72 ± 0.16	-	-	-	6.90
Stage1	5.32 ± 0.11	3.02 ± 0.12	10.0 ± 0.16	-	-	30.0
Stage2	9.06 ± 0.20	2.06 ± 0.05	32.7 ± 0.64	-	-	61.8
Stage3	6.29 ± 0.39	-	44.7 ± 0.86	-	-	49.3
Stage4	8.29 ± 0.17	-	57.1 ± 1.21	-	-	37.2

Table S3 Internal standards for caARG and cfARG.

Internal Standards	**Forward primer (5' to 3')**	**Reverse primer (5' to 3')**	**Annealing temperature (℃)**
caARG, *MHT*	CCCAGATCCCACGGAATCACTT	ATTGCAAAACCATTCCGACCCC	61
cfARG, *ARHGAP11B*	GCCGAGCGGAGTTCAAATTTGA	CGGACACCCTTCACCTTAAT	60

Table S4 The primer sequences and qPCR conditions for all target genes.

Target genes	Forward primer (5' to 3')	Reverse primer (5' to 3')	Annealing temperature (°C)	Reference
*tet*W	GAGAGCCTGCTATATGCCAGC	GGGCGTATCCACAATGTTAAC	60	(Aminov et al., 2001)
*tet*O	ACGGARAGTTTATTGTATACC	TGGCGTATCTATAATGTTGAC	50.3	(Aminov et al., 2001)
*amp*C	CCTCTTGCTCCACATTTGCT	ACAACGTTTGCTGTGTGACG	57.5	(Yang et al., 2012)
*sul*1	CGCACCGGAAACATCGCTGCAC	TGAAGTTCCGCCGCAAGGCTCG	69.5	(Pei et al., 2006)
*sul*2	TCCGGTGGAGGCCGGTATCTGG	CGGGAATGCCATCTGCCTTGAG	65.5	(Pei et al., 2006)
*erm*B	GATACCGTTTACGAAATTGG	GAATCGAGACTTGAGTGTGC	53.5	(Chen et al., 2007)
*erm*F	CGACACAGCTTTGGTTGAAC	GGACCTACCTCATAGACAAG	57.5	Chen et al., 2007)
*bla*OXA1	TATCTACAGCAGCGCCAGTG	CGCATCAAATGCCATAAGTG	60	(Yang et al., 2012)
*int*I1	CTGGATTTCGATCACGGCACG	ACATGCGTGTAAATCATCGTCG	60	(Hardwick et al., 2008)
*tp*614	GGAAATCAACGGCATCCAGTT	CATCCATGCGCTTTTGTCTCT	60	(Zhu et al., 2013a)
*bla*NDM1	CGCCATCCCTGACGATCAAA	CTGAGCACCGCATTAGCCG	57	(Luo et al., 2013)
*rpo*B	AACATCGGTTTGATCAAC	CGTTGCATGTTGGTACCCAT	51	(Dahllof et al., 2000)

Table S5 Primer efficiencies and limit of detection of each assay.

Gene	Efficiency (%)	R^2	Detection limit for influent samples (copies/mL)	Detection limit for effluent samples (copies/mL)
rpoB	103	0.998	231	20
sul1	97.2	0.999	237	20
sul2	90.2	0.998	3070	263
blaOXA-1	107	0.996	35	3
ermF	108	0.993	275	24
tet(W)	112	0.991	102	9
ampC	114	0.998	43	4
ermB	103	0.998	19	2
tet(O)	98.4	0.997	374	32
blaNDM-1	94.1	0.997	282	24
intI1	97.8	0.998	209	18
tp614	95.5	0.998	33	3
iDNA standard	88.9	0.997	175	15
eDNA standard	99.7	0.999	203	17

Table S6 caDNA and cfDNA recoveries of all stages.

Sample		Recovery Efficiency (%)
Baseline – influent	Cell-associated	66.00±25.7
Baseline – effluent	Cell-associated	49.8±41.7
	Cell-free	33.7±7.69
Stage1 - influent	Cell-associated	38.3±10.3
Stage1 - effluent	Cell-associated	78.2±10.2
	Cell-free	31.5±26.2
Stage2 - influent	Cell-associated	56.3±21.9
Stage2 - effluent	Cell-associated	34.4±1.28
	Cell-free	30.7±12.1
Stage3 - influent	Cell-associated	34.0±12.6
Stage3 - effluent	Cell-associated	50.9±20.1
	Cell-free	30.0±7.70
Stage 4 - influent	Cell-associated	77.9±39.0
Stage 4 - influent	Cell-associated	61.1±27.9
	Cell-free	34.4±6.67

Table S7 LRVs of target genes in each operational stage. Influent and effluent concentrations of each gene were significantly different from one another within each stage (t-test, $p<0.001$).

Gene	Baseline	Stage1	Stage2	Stage3	Stage4
intI1	0.21	1.48	2.20	2.43	4.77
sul1	1.44	1.88	3.00	3.05	3.54
sul2	1.28	1.01	2.65	3.13	3.07
ampC	-0.36	0.20	1.36	2.06	2.64
blaOXA-1	2.83	2.22	6.08	3.17	2.21
ermB	3.40	3.35	3.74	4.21	4.04
ermF	3.49	2.20	3.33	3.37	2.44
tet(O)	2.41	2.78	3.98	3.91	3.21
tet(W)	4.63	4.14	2.52	4.22	4.52
tp614	4.18	3.52	4.17	4.40	3.61
blaNDM1	-	-2.18	1.11	1.79	0.88

Table S8 Concentrations of target genes in the influent across all stages (copies/mL of influent).

Target gene	Baseline	Stage 1	Stage 2	Stage 3	Stage 4
*rpo*B	1.32E+05 ± (4.87E+04)	7.95E+05 ± (3.44E+05)	2.79E+05 ± (8.41E+04)	3.83E+06 ± (1.59E+06)	3.22E+06 ± (2.26E+06)
*intI*1	1.47E+07 ± (6.60E+06)	1.08E+08 ± (1.31E+07)	2.53E+08 ± (1.53E+08)	1.15E+08 ± (7.74E+07)	8.38E+07 ± (5.39E+07)
*sul*1	8.23E+07 ± (1.16E+05)	1.42E+08 ± (4.22E+06)	6.62E+08 ± (4.94E+08)	4.85E+08 ± (1.88E+08)	3.04E+08 ± (1.40E+08)
*sul*2	2.23E+06 ± (4.01E+04)	2.93E+06 ± (5.31E+05)	5.04E+07 ± (6.01E+06)	1.05E+08 ± (8.15E+07)	4.46E+07 ± (2.42E+07)
*amp*C	1.18E+05 ± (9.05E+02)	2.41E+06 ± (2.83E+05)	5.12E+06 ± (2.23E+06)	2.46E+07 ± (2.02E+07)	2.01E+06 ± (1.70E+06)
*bla*OXA1	2.59E+04 ± (1.19E+03)	1.11E+04 ± (1.86E+3)	4.71E+06 ± (9.30E+04)	5.44E+06 ± (9.81E+05)	1.28E+06 ± (7.86E+05)
*erm*B	1.34E+06 ± (2.30E+04)	4.62E+06 ± (9.78E+04)	4.71E+06 ± (2.13E+06)	1.25E+06 ± (3.68E+06)	5.88E+05 ± (3.59E+05)
*erm*F	3.07E+06 ± (2.25E+3)	1.32E+06 ± (2.09E+5)	9.91E+06 ± (4.20E+06)	9.07E+06 ± (1.51E+07)	1.73E+06 ± (1.10E+06)
*tet*O	5.66E+06 ± (1.59E+02)	2.35E+06 ± (1.61E+06)	3.34E+07 ± (1.66E+07)	1.87E+07 ± (3.79E+08)	1.26E+07 ± (9.36E+06)
*tet*W	5.71E+06 ± (2.50E+03)	9.94E+06 ± (2.84E+05)	2.87E+06 ± (1.96E+06)	4.61E+08 ± (3.55E+05)	8.44E+06 ± (6.05E+06)
*tp*614	8.42E+06 ± (1.18E+06)	7.30E+05 ± (4.91E+05)	1.23E+07 ± (7.01E+06)	2.05E+07 ± (1.74E+07)	7.72E+06 ± (6.72E+06)
*bla*NDM1	ULC*	4.43E+02 ± (8.17E+00)	1.01E+05 ± (3.92E+04)	1.38E+06 ± (1.17E+06)	5.52E+05 ± (2.57E+05)

Table S9 Concentrations of targeted genes in the effluent across all stages (copies/mL of effluent) in the (a) Cell-associated fraction and (b) cell-free fraction.

Table S9. a

Target gene	Baseline	Stage 1	Stage 2	Stage 3	Stage 4
*rpo*B	6.36E+03 ± (2.83E+03)	1.66E+04 ± (1.96E+04)	1.04E+03± (1.21E+03)	8.62E+03 ± (5.41E+03)	2.42E+02 ± (9.52E+01)
*int*I1	9.07E+06 ± (1.43E+07)	3.57E+06 ± (4.11E+06)	6.67E+05 ± (6.75E+05)	4.51E+05 ± (7.28E+05)	6.43E+02 ± (5.05E+07)
*sul*1	2.50E+06 ± (2.70E+06)	7.31E+05 ± (4.06E+05)	6.08E+05 ± (7.64E+05)	3.18E+05 ± (1.82E+05)	1.04E+03 ± (1.42E+08)
*sul*2	1.13E+05 ± (1.68E+05)	2.76E+05 ± (4.63E+05)	7.08E+04 ± (9.50E+04)	7.40E+04 ± (3.33E+04)	4.24E+03 ± (2.33E+07)
*amp*C	2.74E+05 ± (3.52E+05)	1.52E+06 ± (1.77E+06)	2.22E+05 ± (3.07E+05)	2.14E+05 ± (1.15E+05)	3.45E+03 ± (1.56E+06)
*bla*OXA1	3.65E+01 ± (4.34E+01)	6.49E+01 ± (9.21E+01)	1.97E+00 ± (2.91E+00)	3.63E+03 ± (1.11E+01)	5.57E+01 ± (7.40E+05)
*erm*B	5.18E+02 ± (7.19E+02)	1.86E+03 ± (1.98E+03)	2.55E+02 ± (1.68E+02)	2.90E+01 ± (3.30E+03)	1.49E+01 ± (3.38E+05)
*erm*F	9.91E+02 ± (8.81E+02)	8.13E+03 ± (3.07E+03)	4.59E+03 ± (4.87E+03)	3.87E+03 ± (1.24E+03)	2.46E+01 ± (1.03E+06)
*tet*O	2.15E+04 ± (2.36E+04)	2.89E+03 ± (5.51E+03)	1.99E+03 ± (1.17E+03)	1.57E+03 ± (3.81E+03)	3.81E+02 ± (2.63E+06)
*tet*W	1.07E+02 ± (7.93E+01)	7.01E+02 ± (1.31E+03)	8.51E+03 ± (1.53E+04)	1.12E+04 ± (7.25E+01)	2.24E+01 ± (5.59E+06)
*tp*614	5.39E+02 ± (9.35E+02)	1.20E+02 ± (1.15E+02)	6.55E+02 ± (4.23E+02)	4.17E+02 ± (2.54E+02)	2.14E+02 ± (6.15E+06)
*bla*NDM1	ULC*	6.61E+04 ± (9.66E+04)	7.15E+03 ± (8.92E+03)	2.16E+04 ± (1.19E+04)	1.42E+04 ± (2.59E+05)

Table S9. b

Target gene	Baseline	Stage1	Stage2	Stage3	Stage4
*int*I1	5.91E+02 ± (7.07E+00)	4.58E+03 ± (3.96E+03)	5.79E+03 ± (1.28E+01)	6.50E+01 ± (1.65E+03)	7.90E+02 ± (1.16E+06)
*sul*1	4.98E+05 ± (8.50E+02)	1.15E+06 ± (1.97E+06)	4.88E+04 ± (2.04E+04)	1.15E+05 ± (1.25E+05)	8.62E+04 ± (7.54E+04)
*sul*2	3.08E+03 ± (5.86E+05)	7.21E+03 ± (7.80E+03)	4.19E+04 ± (4.11E+03)	3.99E+03 ± (2.53E+04)	3.32E+04 ± (5.55E+05)
*amp*C	2.46E+01 ± (5.96E+03)	9.27E+03 ± (7.97E+03)	2.25E+03 ± (2.09E+03)	5.35E+02 ± (3.48E+02)	1.12E+03 ± (9.24E+05)
*bla*OXA1	1.45E+00 ± (2.03E+01)	1.75E+00 ± (2.03E+00)	ULC*	2.90E+01 ± (3.50E+02)	7.80E+03 ± (9.70E+03)
*erm*B	1.55E+01 ± (1.29E+01)	1.98E+02 ± (1.90E+02)	6.00E+02 ± (1.78E+01)	4.74E+01 ± (3.54E+01)	3.82E+01 ± (1.33E+01)
*erm*F	1.45E+00 ± (8.69E-01)	1.88E+02 ± (2.41E+02)	1.01E+02 ± (8.01E+01)	1.10E+01 ± (5.55E+02)	6.29E+03 ± (2.53E+03)
*tet*O	3.83E+02 ± (4.70E+02)	1.02E+03 ± (1.41E+03)	1.51E+03 ± (5.68E+01)	7.40E+02 ± (8.89E+03)	7.33E+03 ± (2.60E+03)
*tet*W	2.55E+01 ± (2.30E+01)	1.41E+01 ± (1.38E+01)	8.85E+01 ± (6.01E+01)	1.63E+04 ± (1.12E+01)	2.31E+02 ± (1.65E+02)
*tp*614	2.08E+01 ± (2.88E+01)	9.81E+01 ± (2.53E+02)	1.81E+02 ± (1.56E+02)	4.05E+02 ± (6.01E+10)	1.66E+03 ± (2.82E+03)
*bla*NDM1	ULC*	2.92E+02 ± (4.13E+05)	6.43E+02 ± (5.82E+02)	7.48E+02 ± (3.30E+02)	5.85E+04 ± (4.28E+04)

Table. S10 Relative abundance of ARGs and MGEs normalized by copies of *rpo*B in the influent and the effluent samples across all stages (copies/ copies of *rpo*B): a. influent; b. effluent.

Table S10. a

Target gene	Baseline	Stage1	Stage2	Stage3	Stage4
*int*I1	1.11E+01	1.36E+01	9.08E+01	3.00E+00	2.60E+00
*sul*1	6.22E+01	1.79E+01	2.61E+00	4.23E+00	3.63E+00
*sul*2	1.68E+00	3.69E-01	7.62E-02	2.16E-01	1.47E-01
*amp*C	8.94E-02	3.03E-01	1.02E-01	2.35E-01	4.51E-02
*bla*OXA1	1.95E-02	1.40E-03	9.20E-01	2.21E-01	6.34E-01
*erm*B	1.01E+00	5.81E-01	1.00E+00	2.30E-01	4.61E-01
*erm*F	2.32E+00	1.66E-01	2.10E+00	7.24E+00	2.95E+00
*tet*O	4.28E+00	2.96E-01	3.37E+00	2.06E+00	7.28E+00
*tet*W	4.31E+00	1.25E+00	8.62E-02	2.46E+01	6.68E-01
*tp*614	6.37E+00	9.18E-02	4.29E+00	4.45E-02	9.14E-01
*bla*NDM1	0.00E+00	5.58E-05	8.19E-03	6.75E-02	7.15E-02

Table S10. b

Target gene	Baseline	Stage1	Stage2	Stage3	Stage4
*int*I1	1.43E+02	2.15E+01	6.40E+01	5.23E+00	2.65E-01
*sul*1	3.94E+01	4.40E+00	5.83E+01	3.69E+00	4.30E-01
*sul*2	1.78E+00	1.66E+00	6.79E+00	8.59E-01	1.75E+00
*amp*C	4.31E+00	9.17E+00	2.13E+01	2.48E+00	1.42E+00
*bla*OXA1	5.74E-04	3.91E-04	1.89E-04	4.22E-02	2.30E-02
*erm*B	8.15E-03	1.12E-02	2.44E-02	3.37E-04	6.13E-03
*erm*F	1.56E-02	4.89E-02	4.40E-01	4.50E-02	1.01E-02
*tet*O	3.37E-01	1.74E-02	1.91E-01	1.82E-02	1.57E-01
*tet*W	1.69E-03	4.22E-03	8.16E-01	1.30E-01	9.23E-03
*tp*614	8.47E-03	7.22E-04	6.29E-02	4.84E-03	8.82E-02
*bla*NDM1	0.00E+00	3.98E-01	6.86E-01	2.51E-01	5.87E+00

Table S11 Correlation coefficients for target genes in the effluent cell-associated fraction across all stages, a. r values; b. corresponding p values.

Table S11. a

	rpoB	*intI1*	*sul1*	*sul2*	*ampC*	*blaOXA1*	*ermB*	*ermF*	*tetO*	*tetW*	*tp614*	*blaNDM1*
rpoB	1.00	0.28	0.09	**0.85**	**0.91**	-0.23	-0.09	0.06	-0.04	-0.01	-0.14	**0.93**
intI1	-	1.00	**0.97**	0.39	0.21	-0.34	0.35	-0.11	**0.95**	-0.52	0.17	-0.12
sul1	-	-	1.00	0.26	0.06	-0.30	0.20	-0.17	**0.98**	-0.36	0.40	-0.31
sul2	-	-	-	1.00	**0.97**	-0.18	**0.97**	**0.82**	0.12	-0.26	-0.41	**0.82**
ampC	-	-	-	-	1.00	-0.21	**0.98**	**0.85**	-0.07	-0.29	-0.56	**0.91**
blaOXA1	-	-	-	-	-	1.00	-0.36	0.06	-0.26	**0.73**	0.05	0.00
ermB	-	-	-	-	-	-	1.00	**0.76**	0.07	-0.43	-0.52	**0.84**
ermF	-	-	-	-	-	-	-	1.00	-0.35	0.23	-0.25	**0.81**
tetO	-	-	-	-	-	-	-	-	1.00	-0.41	0.37	-0.40
tetW	-	-	-	-	-	-	-	-	-	1.00	0.51	-0.18
tp614	-	-	-	-	-	-	-	-	-	-	1.00	-0.77
blaNDM1	-	-	-	-	-	-	-	-	-	-	-	1.00

Table S11. b

	rpoB	*intI1*	*sul1*	*sul2*	*ampC*	*blaOXA1*	*ermB*	*ermF*	*tetO*	*tetW*	*tp614*	*blaNDM1*
rpoB	0.00	0.15	0.65	0.00	0.00	0.58	0.64	0.76	0.83	0.01	0.48	0.00
intI1	-	0.00	0.00	0.23	0.38	0.63	0.87	0.95	0.00	0.01	0.97	0.51
sul1	-	-	-	0.52	0.01	0.77	0.83	0.94	0.00	0.00	0.82	0.95
sul2	-	-	-	-	0.00	0.74	0.00	0.01	0.61	0.91	0.34	0.00
ampC	-	-	-	-	-	-	0.00	0.00	0.57	0.98	0.96	0.00
blaOXA1	-	-	-	-	-	-	0.55	0.92	0.68	0.00	0.93	0.99
ermB	-	-	-	-	-	-	-	0.00	0.97	0.75	0.25	0.00
ermF	-	-	-	-	-	-	-	-	0.28	0.56	0.74	0.00
tetO	-	-	-	-	-	-	-	-	-	0.53	0.86	0.39
tetW	-	-	-	-	-	-	-	-	-	-	0.00	0.99
tp614	-	-	-	-	-	-	-	-	-	-	-	0.00
blaNDM1	-	-	-	-	-	-	-	-	-	-	-	0.00

Table S12 Correlation coefficients for target genes in the effluent cell-free fraction across all stages, a. r values; b. corresponding p-values.

Table S12. a

	rpoB	*intI1*	*sul1*	*sul2*	*ampC*	*blaOXA1*	*ermB*	*ermF*	*tetO*	*tetW*	*tp614*	*blaNDM1*
rpoB	1.00	-0.20	0.09	-0.20	-0.21	-0.21	0.47	-0.24	-0.17	**0.77**	-0.09	0.08
intI1	-	1.00	0.29	**0.58**	**0.63**	-0.34	**0.89**	-0.31	-0.21	-0.49	-0.38	-0.33
sul1	-	-	1.00	-0.55	0.83	-0.47	-0.15	-0.33	-0.37	-0.32	-0.45	-0.36
sul2	-	-	-	1.00	-0.12	0.47	0.67	0.47	**0.57**	-0.42	0.46	0.47
ampC	-	-	-	-	1.00	-0.22	0.24	-0.20	-0.17	-0.31	-0.28	-0.22
blaOXA1	-	-	-	-	-	1.00	-0.32	**0.99**	**0.99**	-0.23	**0.98**	0.99
ermB	-	-	-	-	-		1.00	-0.31	-0.19	-0.30	-0.32	-0.32
ermF	-	-	-	-	-		-	1.00	**0.99**	-0.25	**0.97**	**0.99**
tetO	-	-	-	-	-		-	-	1.00	-0.26	**0.97**	**0.99**
tetW	-	-	-	-	-		-	-	-	1.00	-0.04	-0.23
tp614	-	-	-	-	-		-	-	-	-	1.00	**0.98**
blaNDM1	-	-	-	-	-		-	-	-	-	-	1.00

Table S12. b

	rpoB	*intI1*	*sul1*	*sul2*	*ampC*	*blaOXA1*	*ermB*	*ermF*	*tetO*	*tetW*	*tp614*	*blaNDM1*

rpoB	0.00	0.35	0.68	0.37	0.34	0.54	0.02	0.27	0.44	0.00	0.69	0.72
intI1	-	0.00	0.77	0.00	0.00	0.58	0.33	0.00	0.00	0.40	0.00	0.49
sul1	-	-	0.00	0.73	0.75	0.56	0.44	0.70	0.52	0.54	0.80	0.00
sul2	-	-	-	0.00	0.00	0.43	0.36	0.00	0.00	0.49	0.00	0.49
ampC	-	-	-	-	0.00	0.72	0.37	0.00	0.01	0.43	0.00	0.48
blaOXA1	-	-	-	-	-	0.00	0.55	0.00	0.00	0.16	0.00	0.99
ermB	-	-	-	-	-	-	0.00	0.27	0.51	0.05	0.87	0.39
ermF	-	-	-	-	-	-	-	0.00	0.00	0.33	0.00	0.00
tetO	-	-	-	-	-	-	-	-	0.00	0.62	0.00	0.00
tetW	-	-	-	-	-	-	-	-	-	0.00	0.89	0.50
tp614	-	-	-	-	-	-	-	-	-	-	0.00	0.00
blaNDM1	-	-	-	-	-	-	-	-	-	-	-	0.00

Figure Captions

Fig. S1. AnMBR performance throughout all stages. Influent COD, effluent COD, COD removal and methane production are shown. Error bars represent standard deviations of all biological replicates within each stage (n>7 for COD data; n = 3 for methane production of each stage).

Fig. S2 Percent removal contributed by the removal of individual target gene across all operational stages (n=5).

Fig. S3. Concentration of target genes (ARGs and MGEs, copies/mL) in the influent across operational stages (n=5).

Fig. S4 Effluent target gene composition: relative abundance (%) of cell-free target genes and cell-associated target genes (n=5).

Fig. S1

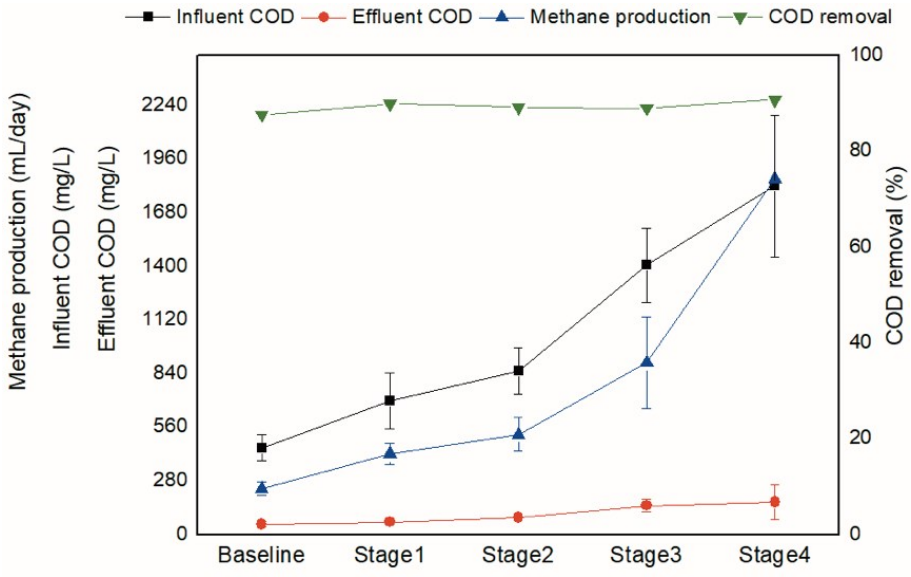
Influent COD
Effluent COD
Methane production
COD removal
Methane production (mL/day)
Influent COD (mg/L)
Effluent COD (mg/L)
COD removal (%)
2240
1960
1680
1400
1120
840
560
280
0
100
80
60
40
20
0
Baseline
Stage1
Stage2
Stage3
Stage4

Fig. S2

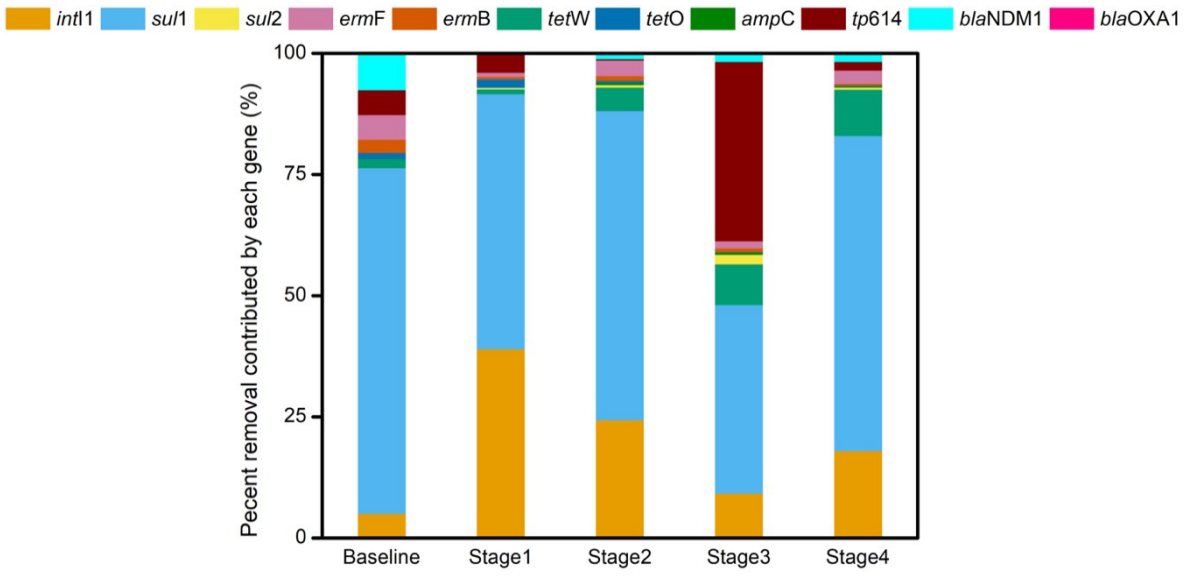
intI1
sul1
sul2
ermF
ermB
tetW
tetO
ampC
tp614
blaNDM1
blaOXA1
Pecent removal contributed by each gene (%)
100
75
50
25
0
Baseline
Stage1
Stage2
Stage3
Stage4

Fig. S3

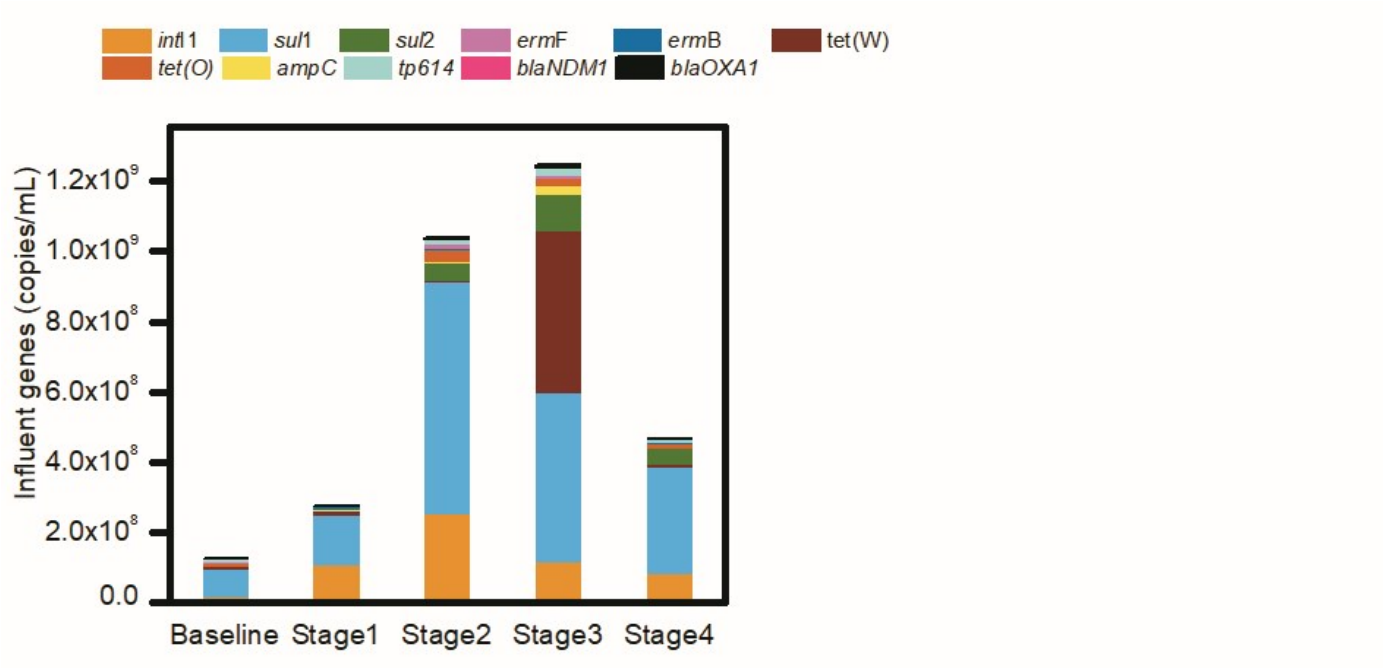
intI1
sul1
sul2
ermF
ermB
tet(W)
tet(O)
ampC
tp614
blaNDM1
blaOXA1
Influent genes (copies/mL)
1.2x10^9
1.0x10^9
8.0x10^8
6.0x10^8
4.0x10^8
2.0x10^8
0.0
Baseline
Stage1
Stage2
Stage3
Stage4

Fig. S4

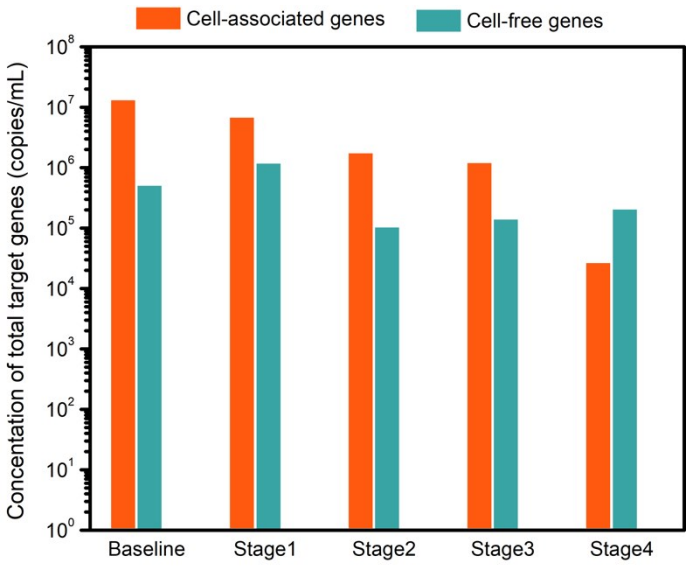
Cell-associated genes
Cell-free genes
Concentation of total target genes (copies/mL)
10^8
10^7
10^6
10^5
10^4
10^3
10^2
10^1
10^0
Baseline
Stage1
Stage2
Stage3
Stage4